

## COB-2019-1431

# THERMOMECHANICAL FATIGUE LIFE OF GRAY AND COMPACTED GRAPHITE CAST IRON ALLOYS

**Douglas Geovanni Bon**

**Márcio Henrique Ferreira, M.Sc.**

**Waldek Wladimir Bose Filho, Dr.**

Department of Materials Engineering, São Carlos School of Engineering, University of São Paulo, 13566-590-São Carlos-SP, Brazil.  
douglas.bon@usp.br marciohenrique@usp.br waldek@sc.usp.br

**Wilson Luiz Guesser, Dr.**

UDESC-CCT, Joinville and R&D Consultant Tupy S.A.- 89227-901 - Joinville, SC - Brazil  
wguesser@tupy.com.br

*The automotive industry has been committed to meet the growing sustainability demands required by the competitive market and by a society concerned to combustion engines energy efficiency as well as a low rate of their components degradation. The ever-growing power density and consequently higher-pressure peaks and temperatures, has demanded cylinder heads and engine blocks with improved mechanical resistance and ductility. The thermo-mechanical fatigue life of cylinder head has been one of the limiting factors in heavy-duty engine design. This work compares the thermomechanical fatigue strength of two cast iron types used for cylinder head fabrication, named as gray cast iron grade 300 (GI300) and compacted graphite cast iron grade 500 (CGI 500). Therefore, out of phase thermomechanical fatigue tests were carried out in temperature range of 50-420°C, considering a trapezoidal wave shape and complete mechanical constraint. By the results, the fatigue strength in the materials lifetime is related to the differences in the graphite cells morphology and their effects as stress concentrators on the pearlitic matrix.*

**Keywords:** gray cast iron, compacted graphite iron, thermomechanical fatigue, cylinder heads.

## 1. INTRODUCTION

Many mechanical and structural components made for application in sectors of aerospace, nuclear, automotive, and oil industries, on numerous occasions, perform activities under severe conditions of temperature and pressure. As an example, are the automotive cylinder heads, which are subjected to sudden temperature and loading variations during the operation period. And the most common material used to make for this kind of application, that require complex geometries, thin sections and, simultaneously, the combination of thermal and mechanical properties to achieve the desired performance are the cast irons [1].

In the cylinder heads of heavy vehicles engines, the valves regions, which are very close together, are heated rapidly by the process diesel combustion and, at the same time, cooled by the cooling system, restricting the material thermal expansion. This results in a high compressive stress state at high temperature, inducing plastic deformations in places where the yield limit has been reached [1]. After the engine shutdown, the temperature drops and tensile stresses are developed as a consequence of the compressive plastic deformations that can generate small cracks and leading to component failure. These internal stresses, generated by the regular engine-working period (start-up, operation and shutdown), reveal a stress-strain hysteresis cycle, called out-of-phase thermomechanical fatigue, OP TMF.



Figure 1: Cylinder head with cracks between valves.

Source: Author.

Seeking for emission reduction as well as higher engine performance, the truck industry is pushing for the development of new diesel engines aiming the enhancement of power density and operation under high peak firing

pressure [2]. However, such power density amplification is also associated with an increased rate of material degradation due to the increased thermal and mechanical loads, which consequently reduces the engine service life. Thus, there is an emerging challenge for heavy-vehicle manufacturers to find material and design solutions from which high engine efficiency can be achieved without compromising the engine durability nor increasing the material or production costs noticeably. There are at present two potential strategies to prolong the service life of engine components. Either the material is replaced with a more resistant substitute, or the component geometry is optimized in order to reduce the intensity of the thermo-mechanical loads at critical locations in the engine. [3].

New grades of cast irons with higher strength have been proposed, opening new alternatives to design engineers. For cylinder heads, the strength requirements are growing continuously in association with good thermal conductivity. In gray irons, the change from the traditional grade GI 250 to the grade GI 300 made it possible to increase the power density of engines. Besides that, the introduction of compacted graphite iron for cylinder heads, starting with grade CGI 450, allowed the use of higher peak firing pressures. The advent of CGI 500, still of restricted use, should bring new design opportunities for both cylinder blocks and heads.

The design of new diesel engines has to consider the complex interaction between microstructure and the mechanical and thermal cycles. Understanding the micromechanisms of damage during OP TMF has still many open questions [4]. According to Löhe et al. [5], multiple mechanisms occur during the OP TMF: plastic deformation, creep, oxidation, strain hardening, nucleation and crack propagation. The cast iron response to these mechanisms depends on another very important factor that is determinant for the component useful life: the morphology, size and distribution of the graphite present in the microstructure.

Academic works to develop new materials of higher strength, are being carried out in many research centers and foundry companies, however in the automotive context, engineers are facing design improvements for engine weight reduction, therefore, the knowledge of the materials' thermomechanical strength, as well as the micromechanisms of failure involved in the cylinder head is of prime concern. These difficulties arise from four main steps of design, that are: the identification of the thermomechanical loadings, the material's mechanical constitutive behavior and its temperature dependence, the damage driving force identification and the fatigue criterion itself [4].

## 2. AIM

The aim of this work is to study the thermomechanical fatigue behavior of two new high-strength cast iron alloys, named as GI300 and CGI 500, gray and compacted graphite cast irons, respectively. High temperature tensile tests were performed to obtain the basic materials tensile properties at different temperatures. After testing the micromechanism of fatigue crack nucleation and growth were evaluated.

## 3. EXPERIMENTAL

### 3.1 Material

The materials investigated in this work were grey cast iron, GI, grade 300 and a compacted graphite cast iron, CGI, grade 500. They are higher strength grades of their families used for cylinder heads. For each family (gray and compacted) the matrix is 100% pearlite, with similar hardness; the main differences are on the graphite size and morphology, shown in figure 2. CGI 500 was Mo alloyed (0,15-0,20%). In GI, the graphite particles are elongated flakes with sharp edges. The graphite particles in CGI are elongated and randomly as in flake graphite iron, however, they are shorter and thicker and have rounded edges [6].

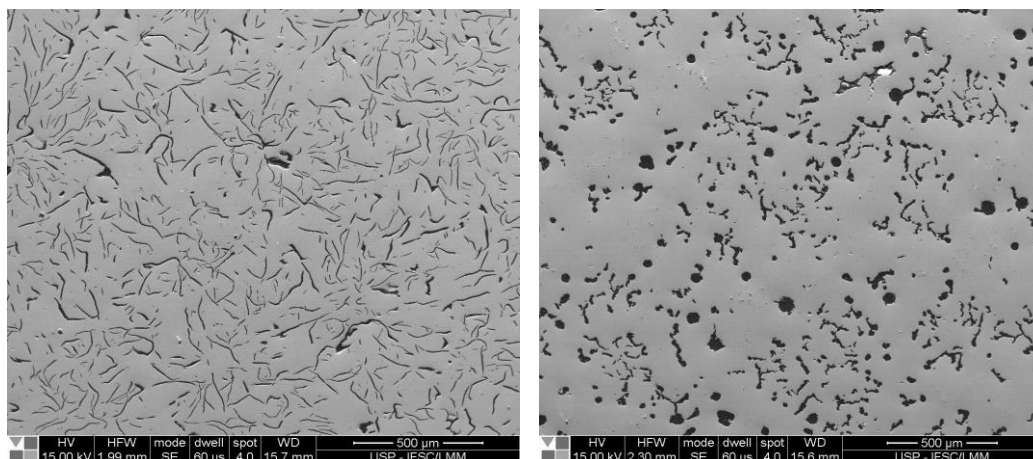


Figure 2: Microstructure GI 300 and CGI 500, respectively.

Source: Author.

Specimens were taken from the cylinder head combustion face of 13 liters, shown in figure 3, with a microstructure as found on the valve bridges regions of this one component. Below, the table I shows the mechanical properties and microstructure characterization of cast irons.

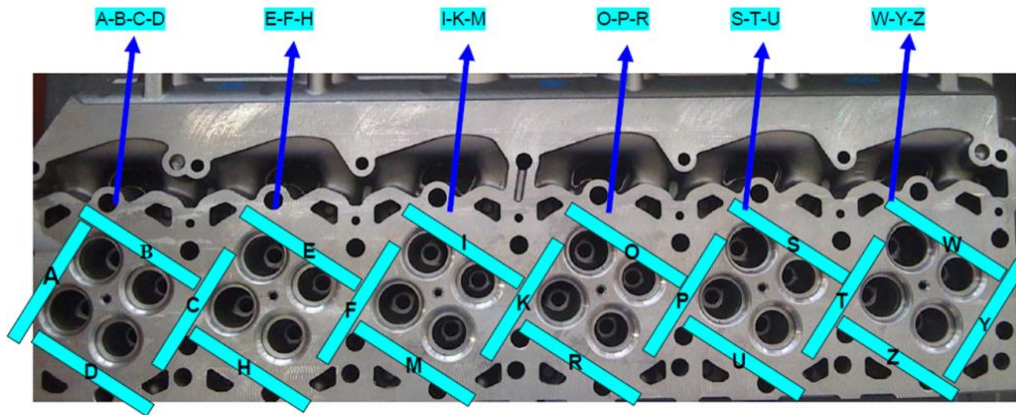


Figure 3: 13 cylinder head and the specimens positions.  
Source: Ghodrati, 2013.

**Table I – Microstructure and mechanical properties (at RT) of the tested materials and base-line cast irons.**

Cast iron	Microstructure	UTS (MPa)	YS (MPa)	E (Gpa)	Cells/cm <sup>2</sup>	Cell size* (μm)	Brinell hardness (HB 5/750)
GI 250 Base-line	Flake graphite, pearlitic matrix	276	227	117	160	676	208
GI 300	Flake graphite, pearlitic matrix	312	285	125	226	569	214
CGI 450 Base-line	Vermicular graphite with 10% nodularity, pearlitic matrix	469	333	150	-	433	221
CGI 500	Vermicular graphite with 22% nodularity, pearlitic matrix	542	360	161	-	337	224

(\*) Using the data from Wimbley [8], the following equation was developed and used to estimate the size of eutectic cells (D) from the number of eutectic cells (N), in gray iron.  $D (\mu\text{m}) = 8547/(N)^{1/2}$ . In CGI the cell size was measured directly.

Source: Tupy S.A.

### 3.2 Out-of-Phase Thermochemical Fatigue Testing

The thermomechanical fatigue tests were performed according to ASTM E2368-17. An MTS servohydraulic fatigue machine (MTS Systems Corporation), model 810, 250 kN capacity, carried out the testings. It was used an extensometer with ceramic rods, model MTS 632.54F14, size of 12mm for axial strain measurement. The heating of the specimens was done using a 7,5 kW high-frequency induction furnace, optical temperature controller on the sample, an infra-red pyrometer and two contact thermocouples (type K) were used. The pressure of the thermocouples is regulated by springs connected. The cooling of the specimens was done by blowing air and by using water-cooled grips. The specimen dimensions followed ASTM E606, with 6 mm diameter and 15 mm gauge length. After machining, they were grounded until #1000 sandpaper. Detailed experimental procedures can be found elsewhere [7]. The specimen size and geometry is presented in Figure 4.

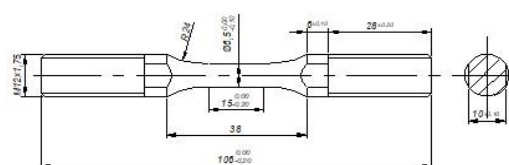


Figure 4: out-of-phase thermomechanical fatigue specimen.  
Available from: ASTM E606-00.

The tests were carried out applying thermal cycles, from 50 and 420°C, with 180s of dwell time at high temperature. The thermal cycle applied is shown in Figure 5.

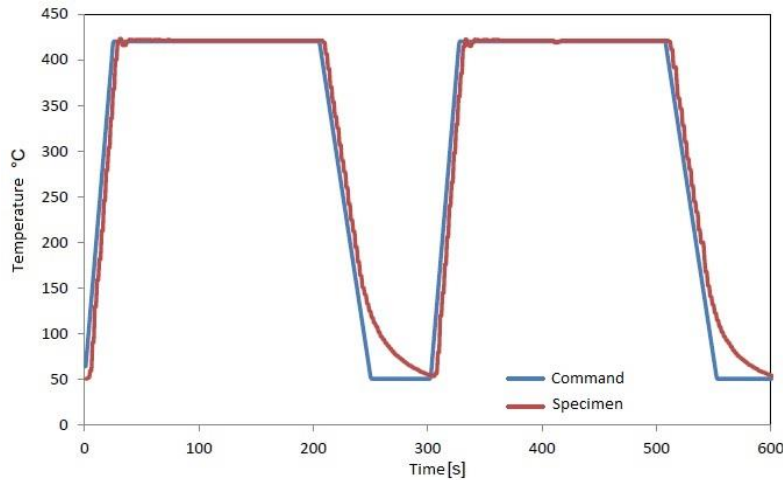


Figure 5: Trapezoidal wavelshape applied in thermomechanical fatigue testing.  
Available from: FERREIRA, 2017.

The OP-TMF tests were performed under full constraint conditions, meaning that the total strain measured by the extensometer was kept constant. This TMF test procedure is intended to replicate the thermal and mechanical conditions in the cylinder heads valve bridge area. For mechanical behavior evaluation, the half-life hysteresis was considered, with life being determined as the number of cycles where the maximum stress drops by 10% or a sudden fracture occurred. Some tests were interrupted to study the microstructural effects on crack initiation and propagation. After testing, the specimen fractured surface was analyzed.

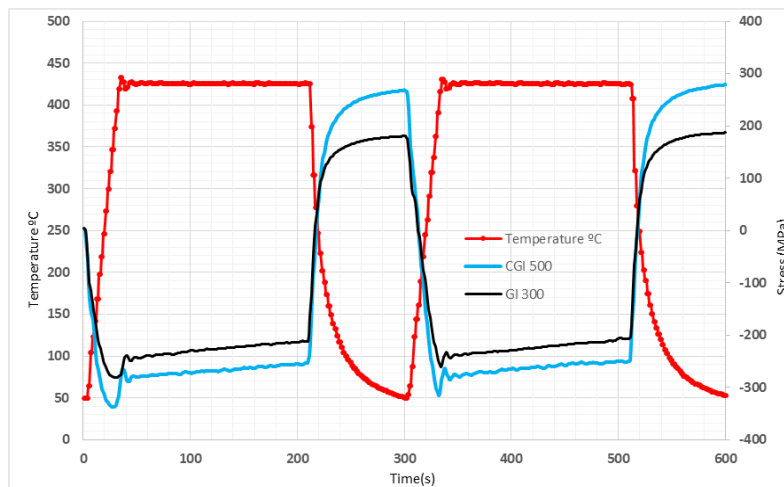


Figure 6: Temperature and stresses evolution during the first two cycles of TMF testing. Example for GI300 and CGI 500.  
Source: Author.

## 4. RESULTS

### 4.1 Out-Phase Thermomechanical fatigue testing

The results of OP TMF testings with the newly developed materials, gray cast iron 300 (GI300) and compacted graphite iron 500 (CGI 500) are listed in table II, also with the results of cast iron baseline, GI 250 and CGI 450, for comparison effect. In this table, the OP TMF lifetime  $N_{10}$  is defined as the number of cycles at which the maximum tensile stress ( $\sigma_{max}$ ) has dropped by 10 percent relative to its maximum value (figure 9). The results of lifetime obtained with CGI are much higher than grey irons, due to the morphology of the graphite, as also reported by Langmayr et al [8]. It's observed an increase of almost 30% on OP TMF lifetime, from GI 250 to GI 300. The increase in lifetime from

CGI 450 to CGI 500 is quite higher, with 193%. We can also observe the higher tensile stresses that CGI can support, compared to grey iron. The difference between the specimens of GI and CGI that shown higher lifetime was 454%.

**Table II. Experimental results for TMF tests based on a circular cross-section of 6.5 mm diameter**

Material	SP	Experimental Values				
		Lifetime N10, cycles	Average Lifetime N10, cycles	Maximum Stress Level (MPa)	Average Stress Level (MPa)	Standard Deviation
GI 250	1	55		234		
	2	112		217		
	3	47	77	212	220	26,8
	4	80		218		
	5	93		219		
GI 300	1	65		225		
	2	97		203		
	3	42	98	235	214	39,8
	4	148		192		
CGI 450	1	180		330		
	2	229		339		
	3	226	223	332	336	31,8
	4	257		344		
CGI 500	1	592		358		
	2	525		363		
	3	680	654	352	355	121,8
	4	820		350		

Source: Author

The increase in the OP-TMF for GI300 is attributed to the refinement and distribution of the graphite. The decrease in size and distribution of eutectic cells on a pearlitic matrix provides greater resistance to crack propagation. The large variance in CGI lifetime is due mainly by changes in the graphite morphology, as the pearlitic matrixes are similar.

Figures 7 and 8 show the Stress versus Mechanical Strain hysteresis loops observed for each material during the OP TMF first and half-life cycle. In the first cycle, during the heating, compressive stresses are generated by the total strain restriction, reaching the yield limit and inducing plastic deformation, as a consequence, the occurrence of stress relieve. At the end of dwell time at maximum temperature, the cooling starts and tensile stresses are developed, with maximum occurring at +50 °C, where the tensile yield limit is reached causing new stress relieving. With cycling, damage evolution takes place and the maximum stress start to decreases and the test is ended when failure criterium is attended (figure 9).

Throughout the test, it is observed the occurrence of cyclic strain hardening in the specimen of CGI (Fig. 8) and consequently the increase in strength.

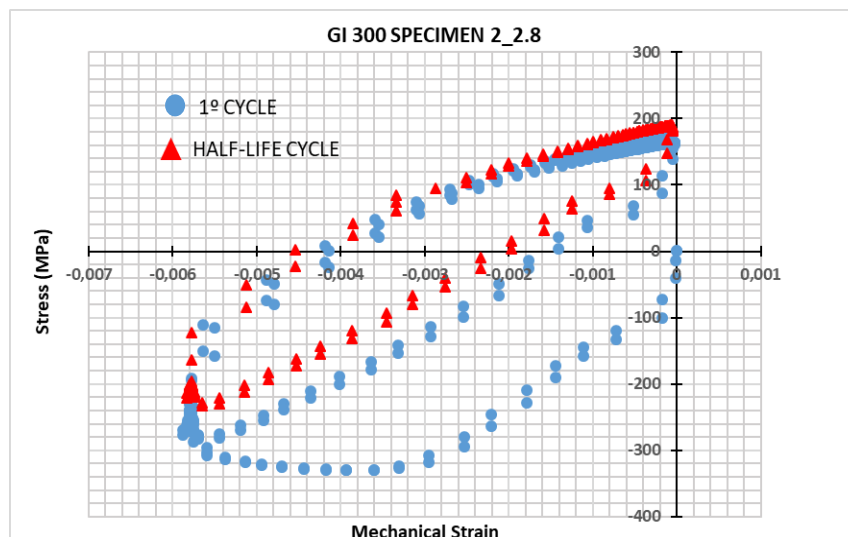


Figure 7: First cycle and half-life cycle for a specimen of GI 300.

Available from: Author.

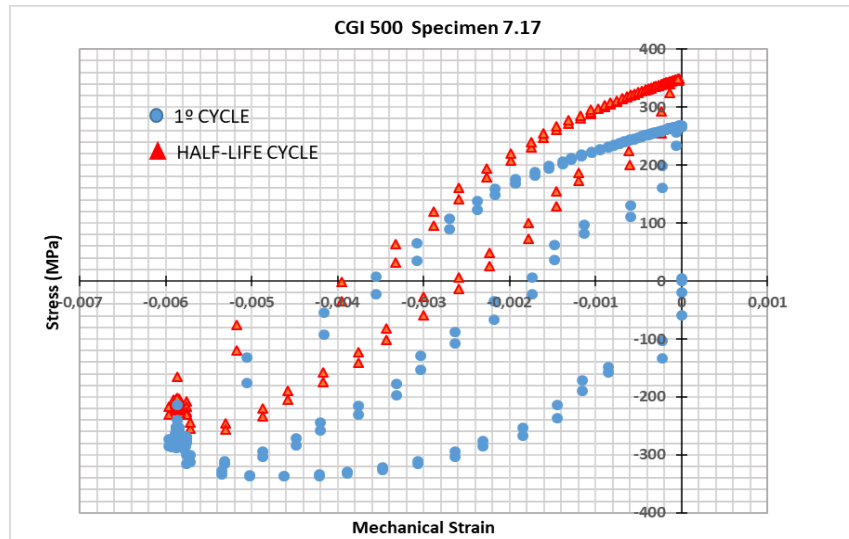


Figure 8. First cycle and half-life cycle for a specimen of CGI 500.  
Available from: Author.

In Figure 9 it is observed an example of the stress evolution during the OP-TMF and the region (arrow) where the adopted failure criterion is reached (10% drop in the maximum tensile stress).

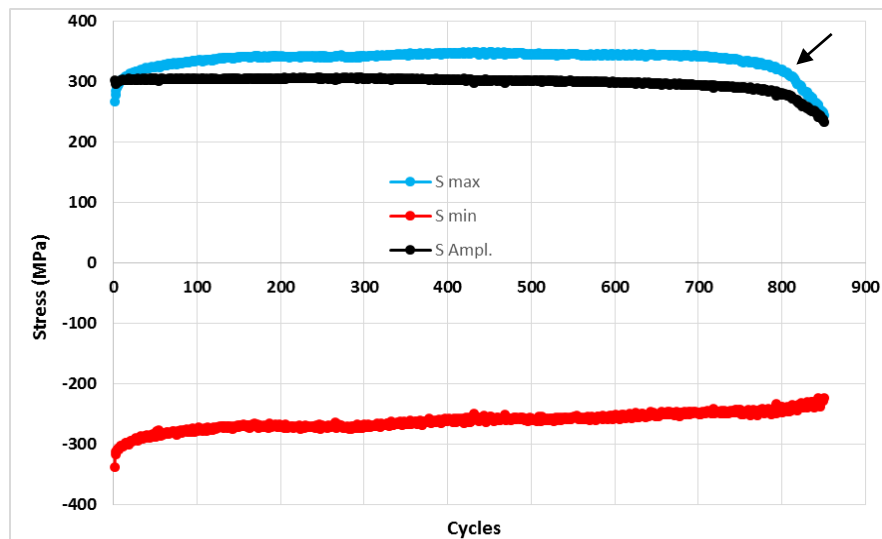


Figure 9: Stresses evolution during OP TMF testing for a specimen of CGI 500.  
Available from: Author.

The process of crack initiation and propagation is similar for gray iron and CGI. Graphite particles play important roles in both steps. The crack starts at graphite tips and growth mainly through the graphite/matrix interface inside an eutectic cell and to move further, the crack has to fracture the matrix between the eutectic cell boundaries. In the cracks linking process, the crack can change direction, following the easier path, growing further into the graphite skeleton, up to the complete specimen fracture.

GI and CGI cast irons can present distinct and particular aspects during this process. In GI, given the higher stress concentration at the graphite tips (needle shape ending), the crack nucleation occurs rapidly at graphite tips, inside the cells or near the specimen surface (less supported region), depending on the local surface conditions. From figure 10, indicated by arrows, it is observed that the cracks are always associated with graphite tips, in some cases connecting to other graphite arms. In CGI the cracks also started at graphite arms (indicated by arrows in figure 11), as reported by Normam et al [9]. The CGI can withstand the presence of a higher number of cracks than GI, before the final fracture, because the crack propagation is more difficult than in gray iron, due to the shape of the graphite (making it like a fingertip), the roughness of the graphite/matrix interface and the space between cells, resulting in a higher life than in gray iron. More detailed information may be found in Bon et. al. (2019) [10].

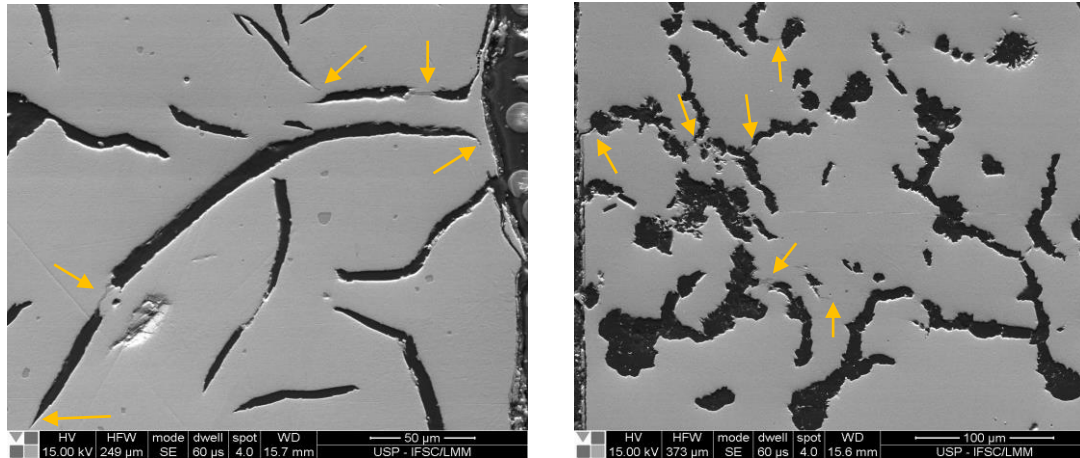


Figure 10: Graphite structure of GI 300 with cracks in tips; Figure 11: Graphite structure of CGI 500 with cracks.  
Source: Author.

## 5. CONCLUSIONS

The results of OP TMF in both cast irons studied here show that:

- The fatigue strength in the materials lifetime is related to the differences in the graphite cells morphology and their effects as stress concentrators on the pearlitic matrix.
- Crack initiation was always associated with graphite particles, in gray iron, and in compacted graphite iron, for all grades.
- An increase of strength in gray iron, from 250 to 300 MPa, results in 30% increase on TMF lifetime, and this is attributed to the refinement of the graphite cells. On the other hand, the effect of increasing strength in CGI, from 450 to 500 MPa, and changes in the graphite arms tips (making it like a fingertip) leads to a significant increase in TMF lifetime (193%) due to retardation in crack initiation.
- Compacted graphite iron sustained higher thermomechanical loadings compared with gray cast iron due to its higher mechanical strength
- GI 300 and CGI 500 has great potential for manufacturing diesel engine components.

## 6. ACKNOWLEDGMENTS

The authors would like to thanks The Brazilian Foundry TUPY for the financial support and for providing the materials, and USP for providing the laboratory facilities. One of the authors would like to thanks The National Council for Scientific and Technological Development, CNPq, Process: Number 306388/2017-0.

## 7. REFERENCES

- [1] Trampert, S., Gocmez, T., G., Pischinger, S. Thermomechanical fatigue life prediction of cylinder heads in combustion engines. *Journal of Engineering for Gas Turbines and Power* 130.1 (2008): 012806.
- [2] Guesser, W. L., Guedes, L. C. The new generation of engines and the challenges for the foundry industry. AEA SIMEA, São Paulo, Brasil, 2016. P. <http://www.proceedings.blucher.com.br/article-details/the-new-generation-of-engines-and-the-challenges-for-the-foundry-industry-23721>
- [3] Fatigue of Heavy-Vehicle Engine Materials Damage Mechanisms, Laboratory Experiments and Life Estimation Viktor Norman.
- [4] Bignonnet, A., and E. Charkaluk. "Thermomechanical fatigue in the automotive industry." *European Structural Integrity Society*. Vol. 29. Elsevier, 2002. 319-330.
- [5] Löhe, D., Tilmann B., Lang, K.H. "Important aspects of cyclic deformation, damage and lifetime behavior in thermomechanical fatigue of engineering alloys." *5th Intern. Conference on Low Cycle Fatigue*. 2003.

- [6] GHODRAT, S. Thermo-mechanical fatigue of compacted graphite iron in diesel engine components. Ph.D Theses. TU Delft, Delft University of Technology. 2013.
- [7] Ferreira, M. H. Análise da vida em fadiga termomecânica de ferros fundidos cinzento e vermicular. Master Thesis, Universidade de São Paulo, São Carlos, 2017.
- [8] Langmayr, F. Zieher, F., Lampic, F. M. Thermomechanik von Gusseisen für Zylinderköpfe. MTZ, p. 298, 4/2004.
- [9] Norman, V., Skoglund, P., Moverare, J. Damage evolution in compacted graphite iron during thermomechanical fatigue testing. Intern. Journal of Cast Metals Research, 2015.
- [10] Bon, D.G., Ferreira, M.H., Bose Filho, W. W., Guesser, W. L. Fracture Micromechanisms Evaluation of High Strength Cast Irons under Thermomechanical Fatigue Conditions. 2<sup>nd</sup> Carl Loper Cast Iron Symposium. Sept 30-Oct 1, 2019 Bilbao, Spain (to be presented).
- [11] E. Charkaluk, A. Bignonnet, A. Constantinescu and K. Dang Van, Fatigue design of structures under thermomechanical loadings, *Fatigue Fracture Engineering Material Structure*, vol. 25, 2002, p. 1199-1206.
- [12] ASTM E2368-10: Standard Practice for Strain Controlled Thermomechanical Fatigue Testing, American Society for Testing of Materials, West Conshohocken, PA, 2004.
- [13] ASTM E606-04 Standard Practice for Strain Controlled Thermomechanical Fatigue Testing, American Society for Testing of Materials, West Conshohocken, PA, 2004.
- [14] GUESSER, Wilson Luiz. *Propriedades mecânicas dos ferros fundidos*. Blucher, 2009.
- [15] REMY, L. Fatigue and thermomechanical fatigue at high temperatures. KH JURGEN BUSCHOW et al. p. 2866-2877, 2001
- [16] Engler-Pinto Júnior, C. C., Spinelli, D.. Fadiga Isotérmica E Termomecânica de uma Superliga À Base De Niquel. *Tecnol. Metal. Mater. Miner.*, São Paulo, v. 11, n. 2, p. 125-130, abr./jun. 2014.
- [17] GHODRAT, S. RIEMSLAG, T. KESTENS, L. PETROV, R. JANSSEN, M. SIETSMA, J. Effects of Holding Time on Thermomechanical Fatigue Properties of Compacted Graphite Iron Through Tests with Notched Specimens. 2012.

## 8. RESPONSIBILITY NOTICE

The authors are the only responsible for the printed material included in this paper.